Am J Transl Res 2021;13(11):12694-12703
www.ajtr.org /ISSN:1943-8141/AJTR0134302

Original Article

MiR-103a-3p aggravates renal cell carcinoma by targeting TMEM33

Jingyu Zhang[1], Qingbo Lu[2], Haigang Pang[3], Min Zhang[4], Wenhai Wei[5]

[1]Department of Urology, The Fourth People's Hospital of Shenyang, Shenyang 110031, Liaoning Province, China; [2]Department of Emergency, Ningyang County First People's Hospital, Tai'an 271400, Shandong Province, China; [3]Department of Urology, The 971st Hospital of Chinese People's Liberation Army Navy, Qingdao 266071, Shandong Province, China; [4]Department of Geriatrics, Sishui County People's Hospital, Ji'ning 273200, Shandong Province, China; [5]Department of Anesthesiology, Shouguang Maternal and Child Care Hospital, Weifang 262700, Shandong Province, China

Received April 15, 2021; Accepted August 31, 2021; Epub November 15, 2021; Published November 30, 2021

Abstract: Objective: We investigated the mechanism of miR-103a-3p-mediated renal cell carcinoma (RCC) progression. Methods: The miR-103a-3p expressions were measured in clinical samples and in two RCC cell lines. MiR-103a-3p was inhibited or over-expressed in the 786-0 and U031 cell lines, respectively. Results: We found that miR-103a-3p is closely related to the development of RCC cells. A bioinformatics analysis and a dual-luciferase reporter gene assay revealed that there is a direct interaction between TMEM33 and miR-103a-3p. Moreover, a rescue assay further confirmed that TMEM33 overexpression can attenuate miR-103a-3p-induced RCC cell development. Conclusion: miR-103a-3p exerts a carcinogenic function in RCC by regulating TMEM33, a finding that may provide new insights into the development of prognostic markers and therapeutic targets for RCC.

Keywords: Renal cell carcinoma, miR-103a-3p, TMEM33, proliferation, metastasis

Introduction

Renal cell carcinoma (RCC) is a urinary system tumor, and it accounts for over 90% of all renal tumors [1]. For RCC without early metastasis, the surgical removal of part or a single kidney is the most effective treatment method, and the patient prognosis is good [2]. Because of the relatively hidden occurrence of RCC, most patients are diagnosed at an advanced stage [3]. Surgical resection is not ideal for RCC patients with metastasis. In addition, RCC is not sensitive to chemotherapy or radiotherapy [4]. Therefore, understanding the molecular mechanisms of RCC pathogenesis is of great importance for finding new therapeutic targets and strategies for RCC.

MicroRNAs are RNAs made up of 20 to 25 nucleotides, and they widely exist in eukaryotes. They regulate post-transcriptional translation by interacting with the 3'-UTR of the targets [5]. The miRNA levels are abnormal in many tumor cells, indicating that miRNAs are implicated in tumor initiation and progression [6]. MiRNAs can participate in the proliferation, invasion, adhesion, metastasis and apoptosis of various solid tumor cells through multiple signaling pathways [7]. For example, miR-1-3p was found to retard the growth of hepatocellular cancer cells through SOX9 [8]. NFIB and CD44 were found to be targets of MiR-302a, which together play an inhibitory role in the progression of colorectal cancer [9]. The growth of osteosarcoma cells can be suppressed by miR-626-3p, and PTN, the target of miR-626-3p, is involved in this process [10]. The combination and interaction of miR-543 and RKIP can accelerate the spread of prostate cancer cells [11]. Hence, miRNAs, as a therapeutic target, may have potential applications in the treatment of RCC.

MiR-103a-3p usually has a very high level in RCC. Existing studies have indicated that miR-103a-3p exerts the opposite effect in various cancers. For example, miRNA-103a-3p promotes the proliferation of human gastric cancer

Table 1. Clinical information of the clinical samples

Items	
Gender	
Male (n)	17
Female (n)	13
Age (years)	
≤60 (n)	12
>60 (n)	18
Tumor size	
≤5 cm (n)	10
>5 cm (n)	20
TNM stage	
T1a (n)	3
T1b (n)	5
T2a (n)	5
T2b (n)	6
T3a (n)	4
T3b (n)	3
T3c (n)	2
T4 (n)	2
Distant metastasis	
Absence (n)	19
Presence (n)	11

cells by targeting and suppressing ATF7 *in vitro* [12]. The inhibition of miR-103a-3p suppresses the proliferation of oral squamous cell carcinoma cells by targeting RCAN1 [13]. In addition, MiR-103a-3p targets the 5' UTR of GPRC5A in pancreatic cells [14].

In this paper, we propose for the first time the mechanism of miR-103a-3p in the progression of RCC. We verified that miR-103a-3p can facilitate the progression of RCC cells by interacting directly with TMEM33 and downregulating its expression. This result provides new directions for research on the mechanism of the occurrence and progress of RCC, and may lead to new research targets for treating RCC.

Materials and methods

Clinical samples

A total of 30 pairs of RCC tissues and para-cancerous tissues were collected from the Fourth People's Hospital of Shenyang from 2019-2020. These tissue specimens were stored in liquid nitrogen prior to the further RNA extraction. The samples' RCC TNM stages were determined based on the 8th edition of AJCC. This research was approved by the Ethics Committee of the Fourth People's Hospital of Shenyang (approval number: SYSY-2018-16). All the patients or their relatives were informed in advance. The detailed clinical information of the samples is shown in **Table 1**.

Cell culture

Human normal kidney cell line HK-2 and RCC cell lines 786-O, UO31 were obtained from ATCC. The cells were inoculated in an RPMI-1640 medium (Sangon Biotech, China) supplemented with 10% FBS (Sangon Biotech, China) and a 1% antibiotic mixture (Sangon Biotech, China), and cultured at 37°C, with 5% CO_2.

Cell transfection

The miR-103a-3p inhibitor (5'-AUACAUUCGCUGUGCACAUCGU-3'), miR-103a-3p mimics (5'-AAGUAGUACACUGCGAAUGUAU-3') and negative control (NC mimics: 5'-UCACAAGCUCAUAGAGAGAUUAGC-3') were synthesized by Sangon Biotech. The vector pcDNA3.1 was purchased from MiaoLing Plasmid Sharing Platform (Hubei, China). The TMEM33 sequence was obtained from NCBI (https://www.ncbi.nlm.nih.gov/), and the open reading frame (ORF) of TMEM33 was amplified by PCR using the cDNA of tissues from clinical samples as template and then inserted into the pcDNA3.1 to construct the TMEM33 expression vector pcDNA3.1-TMEM33. The primers, including the sites of the restriction enzyme used for the construction of TMEM expression vector, were as follows: Forward: 5'-CCGGAATTCAGATGGCATACACCGAGCAAAG-3', Reverse: 5'-CCGCTCGAGTTAGACGACAGTTGGAGCG-3'. The cell transfection was conducted using Lipo3000 (Invitrogen, California, USA) according to the description in the product manual. After 48 h, RT-qPCR and/or Western blot (WB) assays were used to verify the transfection effects. The cells were then used for further experiments.

Real-time quantitative PCR

RNAprep Pure Kits (Tiangen, Beijing, China) were used to extract the total RNA following the instructions in the product manual. SYBR RT-qPCR kits (Tiangen, Beijing, China) and the ABI 7500 System (ABI, USA) were used to quan-

Table 2. The RT-qPCR primer sequences

Gene	Primer Sequences (5'-3')
miR-103a-3p	Forward 5'-AGCAGCATTGTACAGGGCTA-3'
	Reverse 5'-TGGTGTCGTGGAGTCGA-3'
TMEM33	Forward 5'-CGGCAATGTGGCTTTCTCGC-3'
	Reverse 5'-GGGCCAGGAATGCTCTGCTT-3'
U6 snRNA	Forward 5'-CTTAGCAATGCGTTAGATC-3'
	Reverse 5'-ATGGACTATGACGTAGCA-3'
β-actin	Forward 5'-AATGTTACGACAGCTTCGA-3'
	Reverse 5'-CATAAAGCTTACGATCCAAT-3'

tify the miR-103a-3p and TMEM33 levels following to the product manual. The reaction system consisted of 10 μL ddH_2O, 8 μL SYBR, 0.5 μL forward and reverse primers, and a 1 μL sample. The PCR amplification was performed following the PCR amplification procedure: denaturing (95°C, 10 s), annealing (55°C, 15 s), and extension (72°C, 30 s) for 40 cycles. U6 and β-actin were the internal references in this experiment. The relative expression analysis was carried out using the $2^{-\Delta\Delta Ct}$ method. All the primers used are listed in **Table 2**.

Cell proliferation

The cell proliferation was assessed using CCK-8 Kits (Biosharp, Hefei, China) and EdU cell proliferation Kits (Sangon Biotech, Shanghai, China) according to the operating instruction manuals. In detail, the different cell lines were inoculated in 96-well plates at a density of 2×10^3 cells/well and grown to 80% confluence, then 10 μL/well CCK-8 reagent was added, and the cells were cultured at 37°C for another 4 h. The OD450 was measured to determine the cell viability. As for the EdU assays, the cells were first incubated with EdU reagent for 2 h, then immobilized with aldehyde fixative for 30 min and treated with a cell permeability agent for 15 min, and finally stained with DAPI for 30 min. The EdU-stained cells were determined by LSCM (Nikon, Japan), and the proportion of cells stained by EdU was considered to be the cell proliferation rate.

Wound healing assays

786-0 and U031 cells treated with the miR-103a-3p inhibitor or the NC inhibitor were inoculated in 6-well plates until reaching 90% confluence. A 200 μL sterile tip was used to create a wound line in each well, and cell pictures were taken at 0 h and 24 h after the operation.

Transwell migration and invasion assays

Transfected 786-0 and U031 cells were digested and then cultured in a Transwell chamber without Matrigel (Millipore, USA). After incubation for 24 h, the cells in lower chamber were immobilized with an aldehyde fixative for 30 min and incubated with 0.1% crystal violet for 20 min. Finally, the cells were observed and photographed under a microscope. The Transwell invasion assay process was the same as the migration assay, except that the upper Transwell chamber used for the invasion experiment was covered with Matrigel.

Bioinformatics analysis

The ENCORI and miRwalk online analysis systems were used to screen out the target genes of miR-103a-3p that related to RCC. In addition, the binding region of miR-103a-3p and the 3'-UTR of TMEM33 were analyzed using miRwalk.

Western blot

The cells were lysed with a RIPA buffer (Solarbio, China), and the protein content was quantified using BCA Kits (Solarbio, China). The cell lysates were subjected to electrophoresis and film transfer in turn. The film was blocked with BSA and incubated with the primary and secondary antibodies in sequence, and finally developed with the enhanced chemiluminescence reagent ECL (PE0010, Solarbio, China). In this study, all the commercial antibodies were purchased from Abcam, including the primary antibodies: TMEM33 (ab118451, 1:1,000), ITCH (ab245515, 1:2,000), CTTN (ab101359, 1:1,000), SGPP1 (ab108435, 1:500), TAB3 (ab85655, 1:2,000), HADH (ab154088, 1:1,000), β-actin (ab228001, 1:10,000), and the secondary antibody: Goat Anti-Rabbit IgG (ab205718, 1:20000).

Dual-luciferase reporter assays

The fragments of WT and MUT 3'-UTR of TMEM33 containing the putative targeting site of miR-103a-3p were synthesized by Sangon

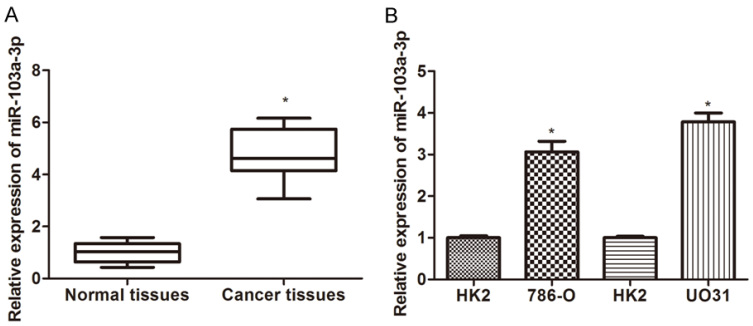

Figure 1. The high expression of miR-103a-3p in RCC. A: The relative level of miR-103a-3p in RCC (n=10) and the neighboring non-cancerous tissues (n=8); B: The relative level of miR-103a-3p in the 786-0, UO31, and HK-2 cells. Compared with the normal tissues or the HK-2 cells group, *P<0.05.

Biotech. Then they were integrated into the dual-luciferase reporter vector (Biovector, China). The MiR-103a-3p/NC mimics and the vector were co-transfected to 786-0 cells and UO31 cells using Lipo3000 Reagent (Invitrogen, CA, USA). After 48 h, the cells' luciferase activity was measured. The relative luciferase activity was calculated using the normalization of the luciferase firefly activities against the Renilla luciferase activities.

Statistical analysis

SPSS 23.0 was used for the statistical analysis. The data are presented as the means ± SD of three parallel experiments. The differences between groups were analyzed using Student's two-tailed *t*-tests or one-way analyses of variance followed by Bonferroni *post hoc* tests. $P<0.05$ was considered statistically significant.

Results

MiR-103a-3p in RCC was significantly up-regulated

First, the relative content of miR-103a-3p in RCC and the para-cancerous tissues were examined. The results showed that the miR-103a-3p in the RCC tissues was much higher than it was in the para-cancerous tissues (**Figure 1A**). Then, the relative content of miR-103a-3p in the three different cell lines was determined. The results were consistent with the results of the RCC tissues, and the miR-103a-3p in the RCC cell lines was much higher than it was in the HK-2 cells (**Figure 1B**). These data indicate that miR-103a-3p may be involved in the occurrence of RCC.

MiR-103a-3p facilitated the progression of RCC cells

To explore the function of miR-103a-3p in RCC cells, a miR-103a-3p inhibitor was introduced into the 786-0 and UO31 cells, respectively. First, we carried out CCK-8 and EdU assays to investigate the role of miR-103a-3p in the proliferation of RCC cells. The data showed that after miR-103a-3p was restrained, the proliferation of the RCC cells was significantly inhibited (**Figure 2A**, **2B**).

Then, we conducted wound healing and Transwell assays to explore the function of miR-103a-3p in the migration and invasion of RCC cells. As shown in **Figure 2C-E**, the migration and invasion abilities of the cells in the miR-103a-3p inhibition groups were remarkably lower than the migration and invasion abilities of the negative control (NC) groups. The above results indicate that miR-103a-3p can facilitate the progression of RCC.

TMEM33 was shown to be the target of miR-103a-3p in the RCC cells

In order to explain the mechanism by which miR-103a-3p promotes the progression of RCC, bioinformatics methods were applied to identify the potential targets of miR-103a-3p. Two online prediction websites (ENCORI and miRwalk) were consulted to identify the candidate targets of miR-103a-3p and a total of 6 target genes were screened out that related to RCC. The relative expressions of the screened 6 genes in the 786-0 and UO31 cell lines were analyzed using RT-qPCR and WB, and we finally chose the down-regulated gene TMEM33 as the object of this study (**Figure 3A**).

To confirm that miR-103a-3p plays an oncogenic role by targeting TMEM33, a Dual-luciferase reporter gene assay was conducted (**Figure 3B**). We transfected the constructed luciferase reporter plasmid and the miR-103a-3p mimics into 786-0 and UO31 cells. The results revealed

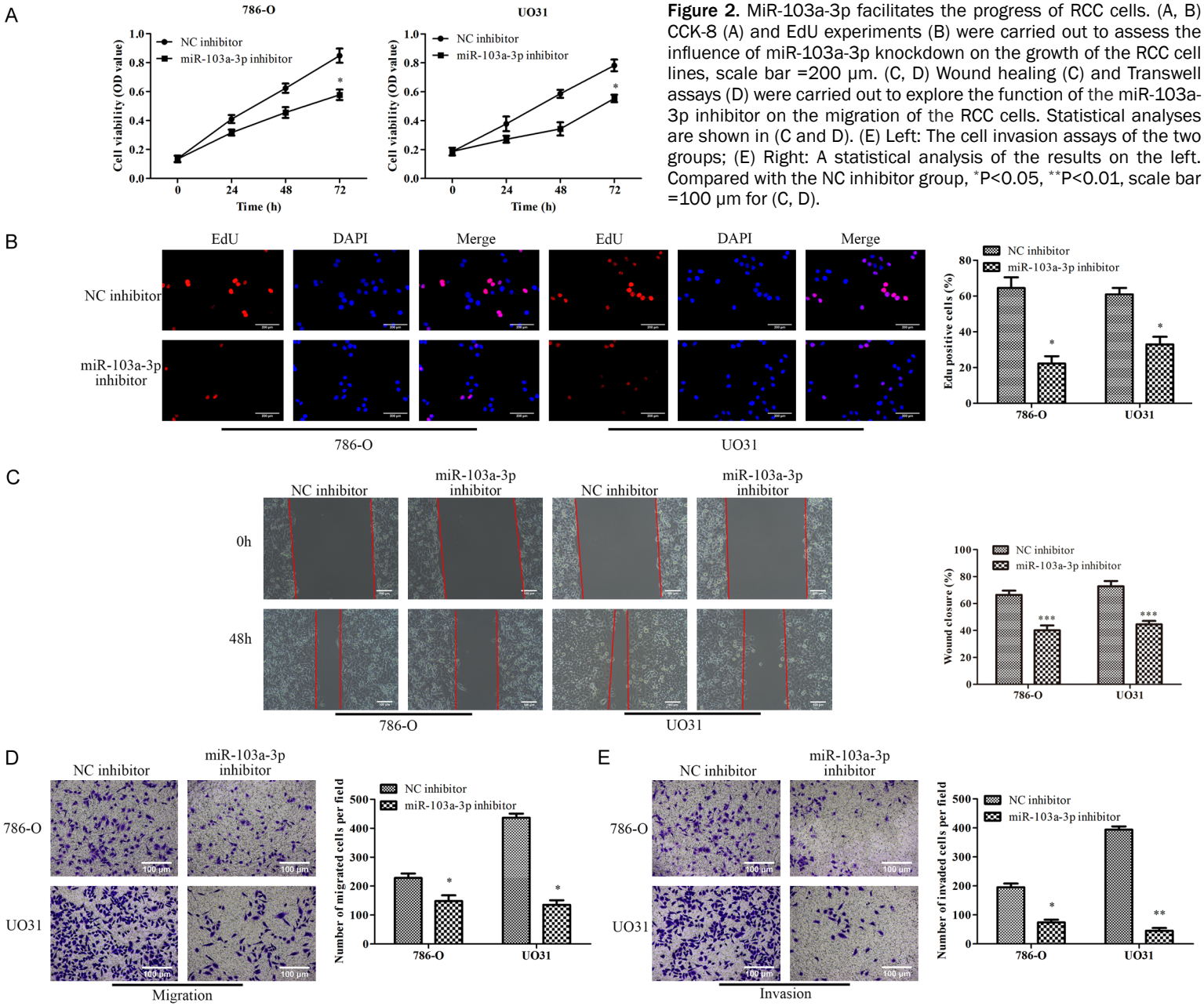

Figure 2. MiR-103a-3p facilitates the progress of RCC cells. (A, B) CCK-8 (A) and EdU experiments (B) were carried out to assess the influence of miR-103a-3p knockdown on the growth of the RCC cell lines, scale bar =200 μm. (C, D) Wound healing (C) and Transwell assays (D) were carried out to explore the function of the miR-103a-3p inhibitor on the migration of the RCC cells. Statistical analyses are shown in (C and D). (E) Left: The cell invasion assays of the two groups; (E) Right: A statistical analysis of the results on the left. Compared with the NC inhibitor group, $^{*}P<0.05$, $^{**}P<0.01$, scale bar =100 μm for (C, D).

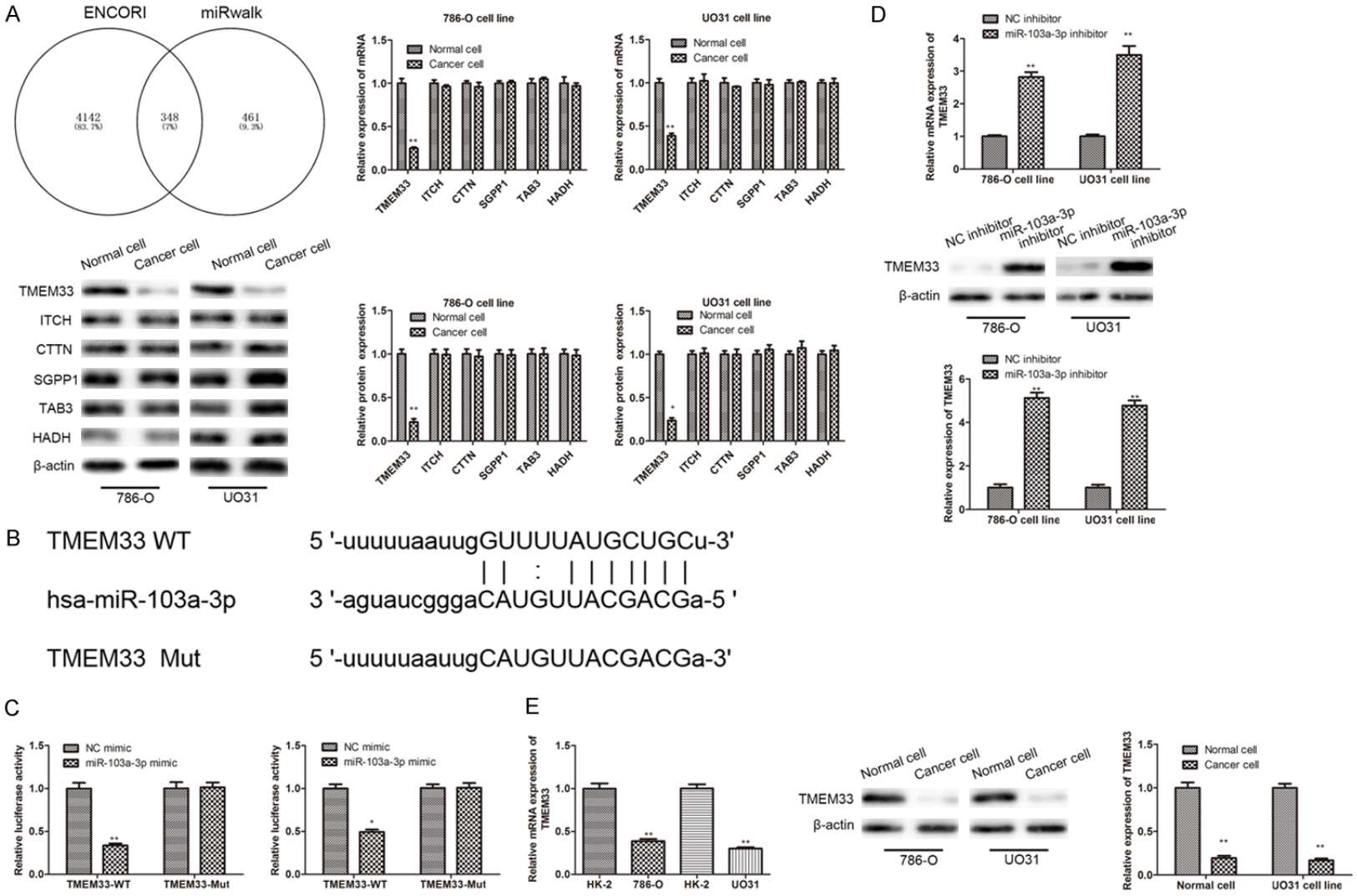

Figure 3. MiR-103a-3p targets and regulates TMEM33 by interacting with the 3'-UTR of TMEM33. A: The ENCORI and miRwalk online prediction websites were used to identify the target genes of miR-103a-3p. RT-qPCR and WB were carried out to determine the relative levels of the screened target genes that relate to RCC. Compared with the normal cell group, **P<0.01; B: Schematic diagram of the luciferase reporter that contains TMEM33-WT or TMEM33-Mut was designed to determine whether miR-103a-3p regulates TMEM33 by interacting with TMEM33; C: A dual-luciferase reporter assay was performed by co-transfecting the miR-103a-3p mimics or the control with a luciferase reporter plasmid including TMEM33 3'-UTR WT or MUT. Compared with the NC mimic groups, *P<0.05, **P<0.01; D: The changes in the relative mRNA expressions of TMEM33 in the 786-O and UO31 cells after miR-103a-3p was inhibited. Compared with the NC inhibitor group, **P<0.01; E: The relative level of TMEM33 in the 786-O, UO31, and HK-2 cells. Compared with the HK-2 cells group, **P<0.01.

that the miR-103a-3p mimics were able to notably suppress the relative luciferase activity of the TMEM33-WT group, but they had little effect on the TMEM33-MUT group (**Figure 3C**). In addition, it was shown that the expression of TMEM33 was remarkably up-regulated in the RCC cells with the inhibited miR-103a-3p (**Figure 3D**). The mRNA and protein expressions of TMEM33 in the 786-0, U031, and HK-2 cells are shown in **Figure 3E**. In short, the above results confirm that miR-103a-3p can target and down-regulate the expression of TMEM33 in RCC.

Over-expression of TMEM33 attenuated the carcinogenic effect of miR-103a-3p in RCC

To explore whether TMEM33 can reverse the carcinogenic effect of miR-103a-3p in RCC, we conducted a rescue assay by over-expressing TMEM33 in the 786-0 and U031 cells. We found that the proliferation-promoting function of miR-103a-3p on the RCC cells was weakened by the overexpression of TMEM33 (**Figure 4A**, **4B**). In addition, the overexpression of TMEM33 significantly attenuated the migration and invasion of the RCC cells induced by the miR-103a-3p mimics (**Figure 4C**, **4D**). In brief, these results suggest that miR-103a-3p exerts an oncogenic effect by targeting and down-regulating the expression of TMEM33.

Discussion

RCC is a urinary system tumor with a high morbidity and mortality [15]. The incidence of RCC is relatively insidious, and most patients are diagnosed at an advanced stage [16]. Therefore, it is of great significance to explore the mechanism of the occurrence and development of RCC. MiRNAs can influence the progression of cancer by regulating the expression of the oncogene and tumor suppressor genes [17]. Many studies have pointed out that miRNAs not only promote the development of tumors, but they also inhibit the development of tumors. In addition, the same miRNA may play opposite roles in different conditions or cells [18].

Existing studies have found that abnormal levels of miR-103a-3p exist in many tumor cells. For instance, Sun et al. found that miR-103a-3p is highly expressed in colorectal cancer cells, and it promoted the proliferation, invasion, migration, angiogenesis, and glycolysis in colorectal cancer via the hippo/YAP1/HIF1A axis [19]. A study by Hu et al. revealed that miR-103a-3p is upregulated in gastric cancer, and it promoted the proliferation of gastric cancer cells by targeting ATF7 [20]. However, miR-103a-3p is not always highly expressed in all cancers. In the research of Ge et al., low levels of miR-103a-3p were found in prostate cancer, and it inhibited the proliferation and invasion of the prostate cancer by targeting TPD52 [21]. Moreover, He et al. also confirmed that a low expression of miR-103a-3p in glioma mediated the expression of ZIC4 and regulated the angiogenesis of glioma [22]. There is still a lack of research and understanding on the levels and functions of miR-103a-3p in RCC. In this research, the results revealed that miR-103a-3p is high-expressed in both RCC tissues and cell lines. The progress of the RCC cells is inhibited by the inhibition of miR-103a-3p, suggesting that miR-103a-3p may play a carcinogenic function in regulating RCC.

TMEM33 is a component of the ER Ca^{2+} signaling machinery required for angiogenesis. The knockdown of TMEM33 overall or specifically to the epithelial cells impairs many downstream effects of VEGF, including the phosphorylation of ERK, notch signaling and vascular development [23]. In addition, TMEM33 was found to be a new molecule that is induced by endoplasmic reticulum stress. It was found that the overexpression of TMEM33 is associated with the enhanced expression of apoptosis signals in breast cancer. In addition, the expression of the autophagy marker LC3II was shown to be increased in TMEM33 overexpressed breast cancer cells, while p62/SQSTM1 is downregulated [24]. In this study, to further illuminate the mechanism by which miR-103a-3p regulates RCC progression, bioinformatics tools were used to analyze the targets of miR-103a-3p. TMEM33 was a screened and verified target of miR-103a-3p. However, the mechanism by which TMEM33 is involved in inhibiting the progression of RCC was not studied in this article, but it will be our future research focus. In addition, our study still lacks *in vivo* validation that the miR-103a-3p/TMEM33 axis promotes the progression of RCC.

In conclusion, our results point out that miR-103a-3p exerts a carcinogenic role by regulat-

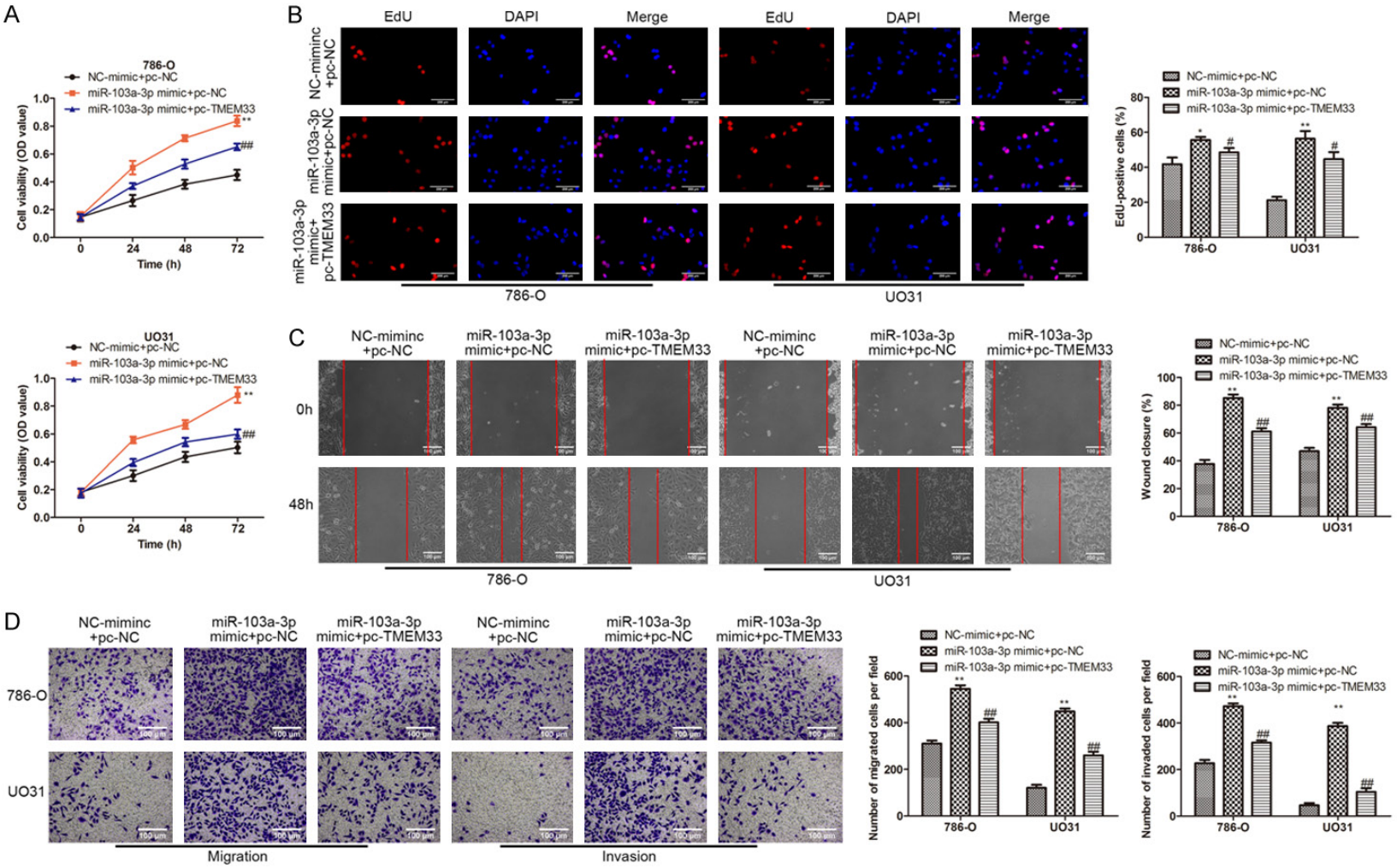

Figure 4. TMEM33 attenuates the carcinogenic effect of miR-103a-3p. 786-O and UO31 cells were transfected with the TMEM33 overexpression vector. Through CCK-8 (A) and EdU assays (B), a wound healing assay (C) and two kinds of Transwell assays (D), the effects of overexpressing TMEM33 on reversing the miR-103a-3p-induced RCC cell development were illustrated. Compared with the NC-mimic+pc-NC group, $^{*}P<0.05$, $^{**}P<0.01$; Compared with the miR-103a-3p mimic + pc-NC group, $^{\#}P<0.05$, $^{\#\#}P<0.01$, scale bar =200 μm in (B), scale bar =100 μm in (C, D).

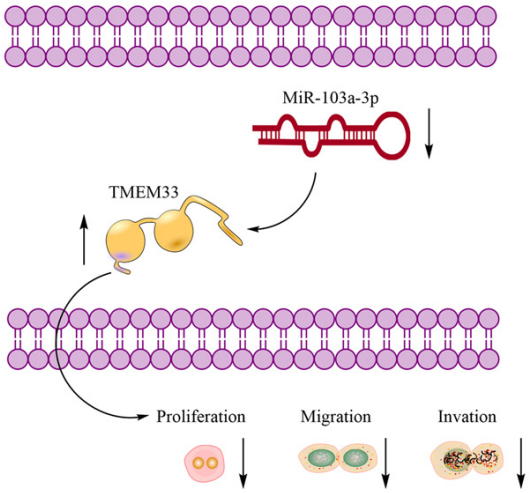

Figure 5. Schematic diagram showing the mechanism of miR-103a-3p in renal cell carcinoma.

ing TMEM33 in RCC. MiR-103a-3p is overexpressed in RCC, and it can accelerate the development of RCC by down-regulating TMEM33 (**Figure 5**). These findings may offer a new way to search for therapeutic targets and potential prognostic markers for RCC.

Disclosure of conflict of interest

None.

Address correspondence to: Haigang Pang, Department of Urology, The 971st Hospital of Chinese People's Liberation Army Navy, No. 22 Minjiang Road, Qingdao 266071, Shandong Province, China. Tel: +86-0532-51840111; E-mail: haigang_pang@tom.com

References

[1] Jonasch E, Gao J and Rathmell WK. Renal cell carcinoma. BMJ 2014; 349: g4797.
[2] Siegel RL, Miller KD and Jemal A. Cancer statistics, 2020. CA Cancer J Clin 2020; 70: 7-30.
[3] Escudier B, Porta C, Schmidinger M, Rioux-Leclercq N, Bex A, Khoo V, Grünwald V, Gillessen S and Horwich A. Renal cell carcinoma: ESMO clinical practice guidelines for diagnosis, treatment and follow-up. Ann Oncol 2019; 1; 30: 706-720.
[4] Kotecha RR, Motzer RJ and Voss MH. Towards individualized therapy for metastatic renal cell carcinoma. Nat Rev Clin Oncol 2019; 16: 621-633.
[5] Dong H, Lei J, Ding L, Wen Y, Ju H and Zhang X. MicroRNA: function, detection, and bioanalysis. Chem Rev 2013; 113: 6207-6233.
[6] Calin GA and Croce CM. MicroRNA signatures in human cancers. Nat Rev Cancer 2006; 6: 857-866.
[7] Lu TX and Rothenberg ME. MicroRNA. J Allergy Clin Immunol 2018; 141: 1202-1207.
[8] Zhang H, Zhang Z, Gao L, Qiao Z, Yu M, Yu B and Yang T. miR-1-3p suppresses proliferation of hepatocellular carcinoma through targeting SOX9. Onco Targets Ther 2019; 12: 2149-2157.
[9] Sun L, Fang Y, Wang X, Han Y, Du F, Li C, Hu H, Liu H, Liu Q, Wang J, Liang J, Chen P, Yang H, Nie Y, Wu K, Fan D, Coffey RJ, Lu Y, Zhao X and Wang X. miR-302a inhibits metastasis and cetuximab resistance in colorectal cancer by targeting NFIB and CD44. Theranostics 2019; 9: 8409-8425.
[10] He M, Shen P, Qiu C and Wang J. miR-627-3p inhibits osteosarcoma cell proliferation and metastasis by targeting PTN. Aging (Albany NY) 2019; 11: 5744-5756.
[11] Du Y, Liu XH, Zhu HC, Wang L, Ning JZ and Xiao CC. MiR-543 promotes proliferation and epithelial-mesenchymal transition in prostate cancer via targeting RKIP. Cell Physiol Biochem 2017; 41: 1135-1146.
[12] Hu X, Miao J, Zhang M, Wang X, Wang Z, Han J, Tong D and Huang C. miRNA-103a-3p promotes human gastric cancer cell proliferation by targeting and suppressing ATF7 in vitro. Mol Cells 2018; 41: 390-400.
[13] Zhang G, Chen Z, Zhang Y, Li T, Bao Y and Zhang S. Inhibition of miR-103a-3p suppresses the proliferation in oral squamous cell carcinoma cells via targeting RCAN1. Neoplasma 2020; 67: 461-472.
[14] Zhou H and Rigoutsos I. MiR-103a-3p targets the 5' UTR of GPRC5A in pancreatic cells. RNA 2014; 20: 1431-1439
[15] Chen ZY, Du Y, Wang L, Liu XH, Guo J and Weng XD. MiR-543 promotes cell proliferation and metastasis of renal cell carcinoma by targeting Dickkopf 1 through the Wnt/β-catenin signaling pathway. J Cancer 2018; 9: 3660-3668.
[16] Shi L, Chen X, Zang A, Li T, Hu Y, Ma S, Lü M, Yin H, Wang H, Zhang X, Zhang B, Leng Q, Yang J and Xiao H. TSC1/mTOR-controlled metabolic-epigenetic cross talk underpins DC control of CD8+ T-cell homeostasis. PLoS Biol 2019; 17: e3000420.
[17] Teoh SL and Das S. The role of MicroRNAs in diagnosis, prognosis, metastasis and resistant cases in breast cancer. Curr Pharm Des 2017; 23: 1845-1859.
[18] Rossi SH, Klatte T, Usher-Smith J and Stewart GD. Epidemiology and screening for renal cancer. World J Urol 2018; 36: 1341-1353.
[19] Sun ZQ, Zhang QG, Yuan WT, Li XL, Chen C, Guo YX, Shao B, Dang Q, Zho QB, Wang QS,

Wang GX, Liu JB and Kan QC. MiR-103a-3p promotes tumor glycolysis in colorectal cancer via hippo/YAP1/HIF1A axis. J Exp Clin Cancer Res 2020; 39: 250.

[20] Hu X, Miao J, Zhang M, Wang X, Wang Z, Han J, Tong D and Huang C. miRNA-103a-3p promotes human gastric cancer cell proliferation by targeting and suppressing ATF7 in vitro. Mol Cells 2018; 41: 390-400.

[21] Ge JY, Mao LK, Xu WQ, Fang WG, Wang NN, Ye DW, Dong Z, Gan H and Cuan C. miR-103a-3p suppresses cell proliferation and invasion by targeting tumor protein D52 in prostate cancer. J Invest Surg 2020: 34: 984-992.

[22] He QR, Zhao LN, Liu XB, Zheng J, Liu YH, Liu LB, Ma J, Cai H, Li Z and Xue YX. MOV10 binding circ-DICER1 regulates the angiogenesis of glioma via miR-103a-3p/miR-382-5p mediated ZIC4 expression change. J Exp Clin Canc Res 2019; 38:9.

[23] Savage AM, Kurusamy S, Chen Y, Jiang Z, Chhabria K, MacDonald RB, Kim HR, Wilson HL, van Eeden FJM, Armesilla AL, Chico TJA and Wilkinson RN. tmem33 is essential for VEGF-mediated endothelial calcium oscillations and angiogenesis. Nat Commun 2019; 10: 732.

[24] Sakabe I, Hu R, Jin L, Clarke R and Kasid UN. TMEM33: a new stress-inducible endoplasmic reticulum transmembrane protein and modulator of the unfolded protein response signaling. Breast Cancer Res Treat 2015; 153: 285-297.